

# SIMULATION OF BEAM-INDUCED GAS PLASMA IN HIGH GRADIENT RF FIELD FOR MUON COLLIDERS\*

K. Yonehara<sup>#</sup>, M. Chung, A. Tollestrup, Fermilab, Batavia, IL 60510, USA

R.P. Johnson, T.J. Roberts, Muons, Inc., Batavia, IL 60510, USA

R.D. Ryne, LBNL, Berkeley, CA 94720, USA

B. Freemire, Illinois Institute of Technology, Chicago, IL 60616, USA

R. Samulyak, Stony Brook University, Stony Brook, NY 11794 and BNL, Upton, NY 11973, USA

K. Yu, Stony Brook University, Stony Brook, NY 11794, USA

## Abstract

A dense hydrogen gas filled RF cavity has been proposed for muon beam phase space cooling and acceleration. The simulation effort has been suggested by the Muon Accelerator Program Advisory Committee (MuPAC) to investigate the characteristic of gas filled RF cavity with intense muon beams. We show the recent experimental result in the gas filled RF test cell and discuss an important gas plasma physics process that we should study in the simulation. Then, we show the present R&D of simulation tool.

## MEASURED PLASMA LOADING

One of critical issues of a high-pressure gas filled cavity is a RF power loading due to beam-induced gas [1]. Incident muons interact with hydrogen gas and produce many electron-ion pairs. Electrons transfer the RF energy into hydrogen gas via the Coulomb interaction. Since the collision frequency is so high ( $10^{13}$  Hz), the ionized electrons reach to equilibrium condition in very short time (0.31-63 ps for RF amplitude 50-0 MV/m in 100 atm hydrogen gas). As a result, the electrons respond the instantaneous value of an external electric field in an RF frequency.

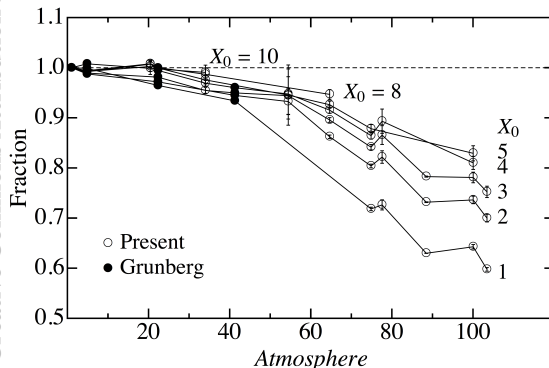


Figure 1: Fraction of measured  $dw$  from the prediction evaluated from Eq. (1).

The RF power loading due to beam-induced gas plasma is formulated based on above assumption. It is given as

$$dw = \iiint 2\pi r \rho(r, z) (\mu_e + \mu_+) E(r, z)^2 \sin^2(\omega t) dt dr dz, \quad (1)$$

\*Work supported by Fermilab Research Alliance, LLC under Contract No. DE-AC02-07CH11359 with the United States Department of Energy.

<sup>#</sup>yonehara@fnal.gov

where  $\mu_e$  and  $\mu_+$  are the mobility of electron and positive ion in hydrogen gas,  $E(r, z)$  and  $\rho(r, z)$  are electric and plasma distributions in the cavity, respectively.  $\mu_e$  and  $\mu_+$  have been measured [2,3] and  $E(r, z)$  and  $\rho(r, z)$  can be estimated from the ionization cooling simulation.

The model was demonstrated in an 805 MHz gas-filled RF test cell (TC) at Fermilab. Figure 1 shows the deviation of measured  $dw$  from the prediction given in Eq. (1) where  $X_0$  is a ratio between RF amplitude and gas pressure. The plot also includes the predicted  $dw$  from the old drift velocity measurement taken in relatively high gas pressure at room temperature by Grunberg [4]. It is clearly seen that there is a big deviation from the prediction at high gas pressure and at low  $X_0$ . This should be gas pressure dependence. We will discuss this effect in later section.

## ELECTRONEGATIVE GAS EFFECT

For the next step, we measured  $dw$  in a small amount of electronegative doped hydrogen gas. We used dry air (DA) that consists of 20 % of oxygen gas.  $O_2$  molecules capture ionized electrons and form a heavy negative ion,  $O_2^-$ . The analytical  $dw$  formula involves the mobility of  $O_2^-$  ( $\mu_-$ ) in  $H_2$  gas,

$$\mu_e + \mu_+ \rightarrow \hat{p}_e \cdot \mu_e + \hat{p}_- \cdot \mu_- + \mu_+, \quad (2)$$

where  $\hat{p}_e$  and  $\hat{p}_-$  are the abundance of electrons and negative ions, respectively (i.e.  $\hat{p}_e + \hat{p}_- = 1$ ).

Figure 2 shows the measured  $dw$  in various DA concentrations in  $H_2$  and  $D_2$  gases as a function of  $X_0$ . A solid line is the prediction where no electron remain in the TC ( $\hat{p}_e = 0$ ) while a broken one is the prediction where no negative ions in the TC ( $\hat{p}_- = 0$ ). At gas pressure 20 atm, the measured  $dw$  is between two lines. It means that there are some residual electrons in the TC. The DA concentration dependence becomes small at gas pressure 75 atm. The electronegative gas effect is saturated at 100 atm. It suggests that the electron capture by  $O_2$  can be taken place via the three-body reaction. We will discuss the reaction in later section. We also operated the TC with DA doped  $D_2$  gas. The measured  $dw$  in  $D_2$  gas becomes smaller than  $H_2$ . Thus,  $D_2$  gas can be a better option than  $H_2$  for the ionization cooling channel.

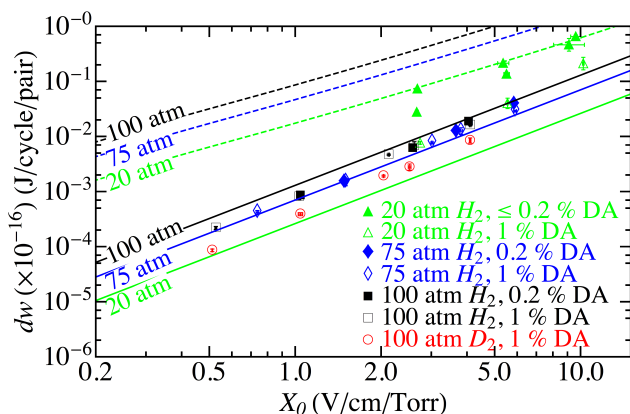


Figure 2: Measured  $dw$  in DA doped  $H_2$  and  $D_2$  gases as a function of  $X_0$ .

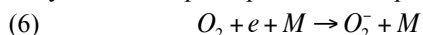
### EXPECTED PLASMA PROCESS

#### Gas Pressure Effect

The Maxwell distribution is used to describe the energy distribution at low  $X_0$  ( $< 0.1$  V/cm/Torr) where the elastic scattering is dominant for the momentum transfer process in a low gas pressure condition. In high gas pressure, the multiple scattering becomes dominant and the energy distribution is deviated from the normal distribution [8]. The multiple scattering model reproduces the measured  $dw$  very well up to 54 atm. However, we saw bigger discrepancy at higher pressure. We should investigate the gas pressure effect in simulation.

#### Three Body Electron Capture Process

The measured  $dw$  in a DA doped  $H_2$  gas suggests that ionized electrons are captured by  $O_2$  via the three-body electron capture process in a very short time. The three-body electron capture process takes place like,



where  $M$  represents any kinds of species, e.g.  $O_2$ ,  $H_2$  ( $D_2$ ), and  $N_2$ .  $M = H_2$  ( $D_2$ ) should be dominant because of large cross-section and abundance in the TC [9].

#### Hydrogen & Ion-Ion Recombination Processes

Ionized electrons can be recombined with positive hydrogen ions. Since a density of  $H_2$  is so large that ionized hydrogen ion immediately forms a polyatomic structure. The abundance of  $H_n^+$  ( $n=3,5,7\dots$ ) should depend on gas and plasma temperatures. There is no theoretical framework to estimate the abundance of  $H_n^+$ . Fortunately, the observed hydrogen recombination rate is so large that  $H_3^+$  should not be dominant in the TC [10]. PIC type simulation is needed to study the recombination process.

Ion-ion recombination process will be complicated because it often requires a multipole interaction, that involves non-linear dynamics. Further study is needed to involve ion-ion process in simulation.

### PRESENT R&D OF SIMULATION TOOL

In this section, we describe a computer code being developed for the simulation of gas filled RF cavities and other problems related to ionization cooling of muon beams and their interaction with plasma in absorbers. The core code uses the particle-in-cell (PIC) method for the Maxwell equations coupled to the dynamics of particles. Particle methods are widely used for the simulation of problems occurring in high energy and nuclear physics, laser and plasmas physics. In our work, we combine electromagnetic PIC methods with probabilistic treatment of atomic physics processes

#### PIC Method for Maxwell's Equations

The system of Maxwell's equations is discretized using the finite difference time domain (FDTD) method on a staggered mesh [7] that achieves second order accuracy in space and time. Electric charges are represented by discrete macroparticles coupled with electromagnetic fields by the action of Lorentz forces and electric currents.

When one solves Maxwell's equations analytically, solving two equations describing the Faraday and Ampere laws is sufficient as the equations expressing the Gauss law and the divergence-free constraint for the magnetic field are invariants of motion. The numerical method of Yee [7] for electromagnetic fields in vacuum also preserves the divergence-free properties of the electric and magnetic fields. To deal with the last two equations in the presence of charges and currents, the rigorous charge conservation method was developed within the PIC framework in [8]. The method calculates electric currents along computational grid edges by solving a geometrical problem of sweeping the computational mesh by finite volumes associated with each macroparticle. By using this method, we find first a set of initial conditions consistent with the Maxwell equations by either solving the Poisson problem for the electric potential or by a superposition of electric fields and changes created by each particle. Then only the first two Maxwell equations and the Newton-Lorentz equation are solved numerically thus avoiding solving the Poisson problem at each time step.

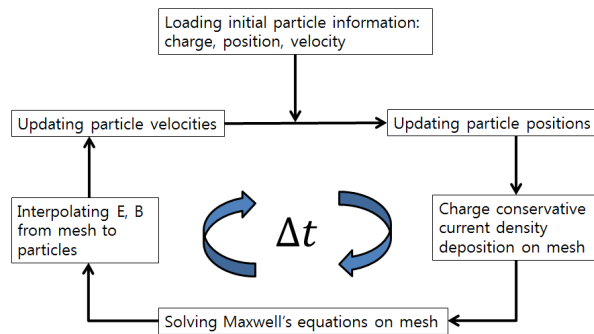


Figure 3: Schematic of time step calculations.

A schematic of processes computed at each time step is depicted in Figure 3. We would like to note that the conservative Leapfrog time discretization scheme for the

Newton-Lorentz equations of particle motion becomes implicit. We use the Boris scheme for the time update [9], which is a modification of the Leapfrog scheme resulting in an explicit and conservative scheme. We also implement modifications of the Boris scheme proposed in [10] for dealing with rapidly accelerating particles for which the relativistic factor  $\gamma$  is not constant.

For accurate simulations of electromagnetic fields in geometrically complex structures, we have implemented the embedded boundary method [11] in a stand-alone Maxwell equation solver. The coupling of algorithms for complex boundaries with the main electromagnetic PIC code will be performed in the next phase.

### *Probabilistic Models for Atomic Physics*

Present work focuses on the implementation of probabilistic models for atomic physics processes in gases under the influence of high energy particles and high gradient electromagnetic fields. As each macroparticle passes through the absorber, it ionizes the medium in real time by creating electron – ion pairs. The motion of ions and electrons is explicitly tracked, and their recombination and other atomic physics transformation are resolved using probabilistic models. The code supports the dynamics of multiple particle species.

### *Code Structure and Properties*

The code is developed in C++ utilizing the advantages of Objected-Oriented Programming. The code is composed of three major parts. The first part, the FieldSolver class, contains FDTD solvers of the Maxwell equations. The second part, the ParticleMover class, contains solvers for the Newton-Lorentz equation. This class also includes various physics models describing particle interactions and transformations by atomic physics processes. The code is capable of tracking numerous particle species. Finally, the third, TimeController class, controls the above classes and any miscellaneous classes such as classes performing the visualization of electromagnetic fields and particle data. The visualization is done using the visualization software called VisIt developed at LLNL for the remote parallel visualization on distributed memory supercomputers. Since the main classes of the code are connected via the interface classes, the code can easily be extended by implementing additional functions and physics models. For convenience of a new problem setup, the initialization routines use XML (eXtensible Markup Language).

### *Parallelization Methods*

The electromagnetic PIC code is parallelized using a hybrid MPI / tread programming for distributed memory multicore supercomputers. The FieldSolver uses a three-dimensional domain decomposition for solving Maxwell's equations. The ParticleMover uses a decomposition of particles that is independent of the FieldSolver domain decomposition. Namely, particles in a parallel computing node can be distributed in the whole computational domain whereas Maxwell's equations are solved in a local

domain of a parallel computing node. As the distribution of particles is usually very non-uniform in the space, such a decomposition maximizes the load balance.

In the electromagnetic-PIC code, computations performed by the ParticleMover are more time consuming compared to computations by the FieldSolver. The described parallel decompositions minimizes the CPU computing time but requires a large amount of communications between the FieldSolver and ParticleMover. We have adopted ideas from the sparse matrix storage to minimize the amount of communications and send field data to ParticleMover from only those computational cells that contain macroparticles.

### *Verification and Validation*

The electromagnetic PIC code has undergone a V&V program and its accuracy and parallel scalability has been estimated. The FieldSolver has been verified using analytical solution for electromagnetic fields in a rectangular cavity. The FieldSolver achieves the second order accuracy and achieves close to linear weak scalability on thousands of processors. The embedded boundary solver has also been verified using analytical solutions for rectangular cavities initialized under some angle to the computational mesh. While the stair-case approximation of boundaries results in a zero-order accuracy, the use of the embedded boundary method restores the accuracy to the order of 1.4 – 1.5. The ParticleMover has been verified using space charge problems and problems with special distributions of particles. Probabilistic models for atomic physics will be validated by simulating experiments on beam-induced plasma in high gradient RF cavities.

## ACKNOWLEDGEMENT

We thank to Vladimir Shiltsev and Mark Palmer for supporting this program.

## REFERENCES

- [1] K. Yonehara et al., Proceedings of IPAC 2013, TUPFI059.
- [2] J.J. Lowke, Aust. J. Phys. 16, 115 (1962).
- [3] T.M. Miller et al., Phys. Rev. 173, 115, 1968.
- [4] R. Grunberg, Z. Physik 204, 12, 1967.
- [5] T.T. O'Malley, J. Phys. B: Atom. Molec. Phys. 13, 1491, 1980.
- [6] B. Freemire et al., Proceedings of IPAC 2013, TUPFI064.
- [7] K. Yee, IEEE Transactions on Antennas and Propagation, 14 (3) (1966) 302-307.
- [8] J. Villasenor and O. Buneman, Comput. Phys. Commun., 69 (1992) 306-316.
- [9] J. Boris, Proc. 4th Conf. on Numer. Simulation of Plasmas, Washington DC, NRL, 1970, 3-67
- [10] J. L. Vay, Physics of Plasmas, 15 (2008), 056701.
- [11] S. Dey, R. Mittra, IEEE Microwave and Guided Wave Letters, 7 (1997), 273-275.